Impact of reionization on CMB polarization tests of slow-roll inflation

Michael J. Mortonson[1,2] and Wayne Hu[1,3]

[1]*Kavli Institute for Cosmological Physics, Enrico Fermi Institute, University of Chicago, Chicago, IL 60637*
[2]*Department of Physics, University of Chicago, Chicago, IL 60637*
[3]*Department of Astronomy and Astrophysics, University of Chicago, Chicago, IL 60637*
(Dated: October 22, 2007)

Estimates of inflationary parameters from the CMB B-mode polarization spectrum on the largest scales depend on knowledge of the reionization history, especially at low tensor-to-scalar ratio. Assuming an incorrect reionization history in the analysis of such polarization data can strongly bias the inflationary parameters. One consequence is that the single-field slow-roll consistency relation between the tensor-to-scalar ratio and tensor tilt might be excluded with high significance even if this relation holds in reality. We explain the origin of the bias and present case studies with various tensor amplitudes and noise characteristics. A more model-independent approach can account for uncertainties about reionization, and we show that parametrizing the reionization history by a set of its principal components with respect to E-mode polarization removes the bias in inflationary parameter measurement with little degradation in precision.

I. INTRODUCTION

Temperature and polarization power spectra of the cosmic microwave background (CMB) are consistent with predictions of the simplest inflationary models [1–4]: a nearly flat geometry, superhorizon correlations as probed by the spectrum of acoustic peaks, and primordial scalar perturbations that are adiabatic, Gaussian, and close to scale-invariant [5–9]. One of the key remaining signatures of inflation, tensor perturbations (i.e. gravitational waves) [10, 11], has yet to be detected. Depending on the amplitude of the tensor perturbations, which is not well constrained theoretically, it may be possible to measure the angular power spectrum of the inflationary gravitational waves in the B-mode component of the CMB polarization on large scales. Non-detection of the tensor spectrum does not necessarily rule out inflation, but upper limits on r can be used to exclude particular models of inflation and limit its energy scale. Many experiments have been proposed to search for this signal [12–21].

Measurement of tensor perturbations in the B-mode polarization power spectrum would test models of inflation by constraining inflationary parameters. These parameters include the tensor-to-scalar ratio, r, and the tensor spectral index, n_t, which are related by a consistency relation under the simplest single-field slow-roll inflationary scenarios. If the tensor spectrum can be detected, precise measurements over a wide range of scales could test the consistency relation.

CMB constraints on r and n_t depend on the ability to accurately determine the large-scale power in B-modes due to tensor perturbations, independent of the effects of other cosmological parameters. On the largest scales, the tensor B-mode spectrum depends not only on inflationary parameters but also on the reionization history of the universe [22]. The main impact of reionization on the spectrum is through the total optical depth, τ. The 3-year *WMAP* measurements of E-mode polarization determine τ to an accuracy of about 30% [9, 23], and future CMB experiments should constrain τ at the $5 - 10\%$ level [12, 24–26].

However, the detailed evolution of the reionization history also significantly affects the large-scale polarization spectra. Uncertainty in this history leads to added uncertainty in inflationary parameters. Moreover, incorrect inferences due to an oversimplified treatment of reionization may bias estimates of inflationary parameters. For unbiased estimation of the optical depth from the E-mode reionization peak, the solution is to use a complete, principal-component-based description of reionization effects when estimating parameters from CMB polarization data [25, 27]. In this paper, we extend this approach to tensor B-mode polarization and show that it is equally if not more effective in ensuring accurate measurements with little loss in precision.

The outline of the paper is as follows. We discuss the effects of reionization and inflationary parameters on the polarization power spectra and the large-scale degeneracy between these parameters in § II. A brief overview of the principal component parametrization of the reionization history follows in § III. In § IV, we describe our Markov Chain Monte Carlo analysis of simulated polarization data and give the resulting constraints on τ, r, and n_t, which we discuss further in § V.

II. POLARIZATION DEPENDENCE ON REIONIZATION AND INFLATIONARY PARAMETERS

Like the scalar E-mode polarization power spectrum, the tensor B-mode spectrum $C_\ell^{BB,\mathrm{T}}$ consists of two main components: one from recombination that peaks at $\ell \sim 100$, and the other from the epoch of reionization, which peaks near $\ell \sim 5$ and dominates at $\ell \lesssim 20$ (Fig. 1). In the tensor power spectrum, these components arise from wavenumbers $k \sim 0.01$ Mpc^{-1} and ~ 0.0007 Mpc^{-1} respectively. They provide a lever arm of over a decade in physical scale for measuring the tensor tilt. This lever arm is slightly shortened compared with the ratio of an-
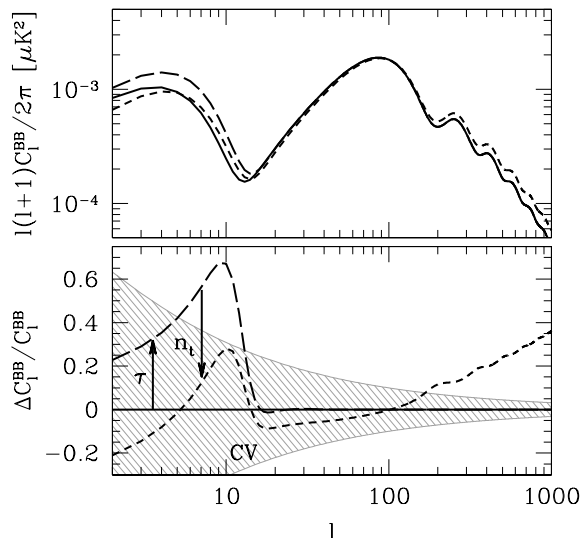
FIG. 1: *B*-mode tensor spectra illustrating the degeneracy between τ and n_t for large-scale measurements, with angular power spectra plotted in the upper panel and fractional deviations from the base model in the lower panel. For the base model (*solid*), $r = 0.03$, $\tau = 0.1$, and $n_t = -0.00375$. The other two models have $\{\tau, n_t\} = \{0.12, -0.00375\}$ (*long dashed*) and $\{0.12, 0.13\}$ (*short dashed*), with a pivot scale of $k_{\mathrm{pivot}} = 0.01$ Mpc^{-1}. The reionization history here is assumed to be instantaneous. Cosmic variance of $C_\ell^{BB,\mathrm{T}}$ for the base model, which excludes the variance from lensing, is shown by the shaded band in the lower panel.

gular scales due to the closer distance to reionization. Nonetheless, these features provide an opportunity to test the slow-roll inflationary consistency relation [e.g., 28],

$$n_t = -r/8, \qquad (1)$$

between the tensor-to-scalar ratio r and tensor tilt n_t. Deviations from the consistency relation and running of the tilt come in at second order in the slow-roll parameters. Specifically, r is four times the ratio of the tensor power spectrum amplitude (for one component of gravitational waves) to the scalar curvature power spectrum amplitude, in accordance with the definition used by CAMB and *WMAP*.

Note that we quote r at a normalization scale of $k_{\mathrm{pivot}} = 0.01$ Mpc^{-1} whereas 3-year *WMAP* results quote it at $k_{\mathrm{pivot}} = 0.002$ Mpc^{-1} and CAMB defaults to $k_{\mathrm{pivot}} = 0.05$ Mpc^{-1}. Our choice, corresponding to the recombination peak at $\ell \approx 100$, better reflects the scale at which the tensor spectrum can be best measured. We will use subscripts to denote choices of scale other than 0.01 Mpc^{-1}, e.g. $r_{0.05}$ for normalization at $k_{\mathrm{pivot}} = 0.05$ Mpc^{-1}, so that

$$r_{k_{\mathrm{pivot}}/\mathrm{Mpc}^{-1}} = r\left(\frac{k_{\mathrm{pivot}}}{0.01\ \mathrm{Mpc}^{-1}}\right)^{n_t+1-n_s}, \qquad (2)$$

assuming no running of the scalar or tensor spectral indices. Since we only consider small deviations from scale-invariance, the tensor-to-scalar ratio varies little with the normalization scale so any corrections to Eq. (1) due to changing k_{pivot} are correspondingly small.

Cosmic variance and reionization history uncertainties in the interpretation of the reionization peak limit the ability to measure the spectrum from this technique. In Fig. 1, we show that variation in the optical depth to reionization, τ, can mimic changes to n_t within the precision of cosmic variance of the individual ℓ modes,

$$\frac{\Delta C_\ell^{BB,\mathrm{T}}}{C_\ell^{BB,\mathrm{T}}} \approx \sqrt{\frac{2}{2\ell+1}}. \qquad (3)$$

The example of Fig. 1 shows that there are at least two ways of breaking this degeneracy. One is by measuring the tensor spectrum at $\ell > 100$, where the tilt of the spectrum matters but the optical depth has no effect other than an overall rescaling of the spectrum by $e^{-2\tau}$, which we absorb by changing the scalar amplitude A_s to keep $A_s e^{-2\tau}$ fixed. Just as in the scalar case, if the tensor spectrum can be precisely measured beyond the recombination peak, the global constraint on n_t will not be sensitive to reionization. Unlike the scalar case, $C_\ell^{BB,\mathrm{T}}$ falls sharply at higher ℓ and becomes masked by *B*-modes generated by lensing of *E*-modes [29] ($C_\ell^{BB,\mathrm{L}}$; see Fig. 2). The power in the lensing *B*-modes is expected to be greatest at $\ell \sim 1000$, a smaller scale than the reionization and recombination peaks of the tensor spectrum. The relative amplitude of the tensor and lensing contributions to C_ℓ^{BB} depends on the tensor-to-scalar ratio, which the 3-year *WMAP* data restrict to $r \lesssim 0.3$ [9].

If r is near the current upper limits, the lensing spectrum can be statistically subtracted to a large extent. Nevertheless, instrumental and foreground limitations may still prevent the extraction of information from scales beyond the recombination peak for next generation experiments such as *Planck* [30–33]. At much lower r, the best CMB constraints on n_t will come from the combination of the recombination and reionization peaks unless the lensing signal can be subtracted directly from the polarization maps [34–38].

The $\tau - n_t$ degeneracy is also broken through the constraint on τ from the *E*-mode reionization peak, which depends on τ but not n_t as long as r is small enough that C_ℓ^{EE} is dominated by scalar perturbations. To break the degeneracy in this way, it is important to have accurate constraints on τ that do not depend on overly simplistic assumptions about the reionization history.

The shape of the reionization peak depends on the history of the spatially-averaged ionized fraction, $x_e(z)$. In Fig. 2, we illustrate two models with similar optical depths but different reionization histories. A model-dependent analysis of the polarization power spectrum that uses an incorrect form of $x_e(z)$ can result in significant bias in the total optical depth to reionization [24, 25, 39, 40]. To the extent the constraint
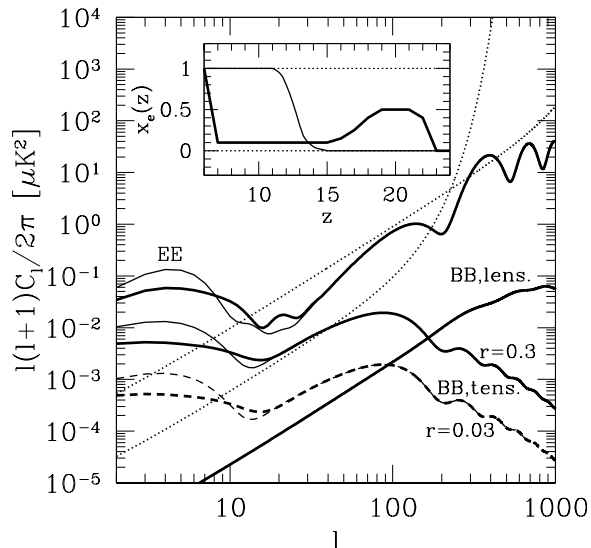
FIG. 2: E- and B-mode polarization angular power spectra and reionization histories (*inset*) for an extended, "double" reionization history with $\tau = 0.090$ (*thick curves*) and a nearly-instantaneous reionization model with optical depth $\tau = 0.105$ (*thin*). For the B-modes, both the tensor spectra [with tensor-to-scalar ratio $r = 0.3$ (*solid*) and $r = 0.03$ (*dashed*)] and lensing spectra are plotted. Dotted curves are the assumed *Planck* and *CMBPol* noise power spectra, from top to bottom at low ℓ respectively.

on n_t relies on measurements of the reionization peak of $C_\ell^{BB,\mathrm{T}}$, it may be biased as well in such an analysis. We shall see that the use of model-independent principal components of the reionization history protects against such biases at little cost to the precision of the inflationary test.

III. PRINCIPAL COMPONENT PARAMETRIZATION OF REIONIZATION

Following [25, 27], we parametrize the reionization history as a free function of redshift by decomposing $x_e(z)$ into its principal components with respect to the E-mode polarization of the CMB:

$$x_e(z) = x_e^{\mathrm{fid}}(z) + \sum_\mu m_\mu S_\mu(z), \qquad (4)$$

where the principal components, $S_\mu(z)$, are the eigenfunctions of the Fisher matrix that describes the dependence of C_ℓ^{EE} on $x_e(z)$, m_μ are the amplitudes of the principal components for a particular reionization history, and $x_e^{\mathrm{fid}}(z)$ is the fiducial model at which the Fisher matrix is computed. In practice, we construct the principal components assuming E-mode information only by taking the tensor-to-scalar ratio $r = 0$. For allowed values of r, the information on the ionization history from the tensors is subdominant to the scalars. The inverses

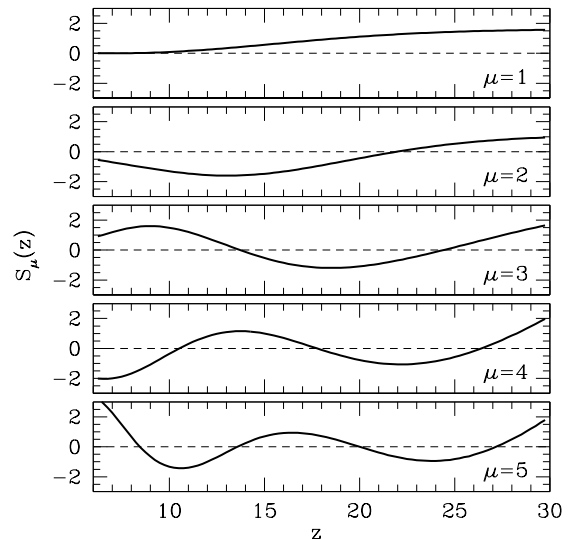

FIG. 3: The five lowest-variance principal components of $x_e(z)$ over redshifts $6 < z < 30$, with increasing variance from top to bottom.

of the eigenvalues of the Fisher matrix give the estimated variances of the principal components, σ_μ^2, which determine the ordering of the components by requiring that $\sigma_\mu^2 < \sigma_{\mu+1}^2$. The main advantage of using principal components as a basis for $x_e(z)$ is that only a small number of the components are required to completely describe the effects of reionization on large-scale CMB polarization, so we obtain a very general parametrization of the reionization history at the expense of only a few additional parameters.

The principal components are defined over a limited range in redshift, $z_{\mathrm{min}} < z < z_{\mathrm{max}}$, with $x_e = 0$ at $z > z_{\mathrm{max}}$ and $x_e = 1$ at $z < z_{\mathrm{min}}$. We take $z_{\mathrm{min}} = 6$, $z_{\mathrm{max}} = 30$, and constant $x_e^{\mathrm{fid}}(z) = 0.15$ here, and refer to [25] for further discussion of the choices of these and other parameters related to the principal components.

For complete representation of the effects of reionization between z_{min} and z_{max} on the low-ℓ E-mode spectrum to better accuracy than cosmic variance, no more than the first five principal components are needed (assuming $z_{\mathrm{max}} \lesssim 30$) [25, 27]. Due to projection effects [41], the accuracy to which the lowest-variance principal components reconstruct $C_\ell^{BB,\mathrm{T}}$ at low ℓ is even better than for the scalar C_ℓ^{EE}. In the MCMC analysis presented in the following section, we always use the five lowest-variance principal components of $x_e(z)$ with $z_{\mathrm{max}} = 30$, which we show in Fig. 3 (see [25] for the effects of using a different number of components to analyze E-mode data). The amplitudes of these components then serve to parametrize general reionization histories in the analysis of CMB polarization data.

IV. MARKOV CHAIN MONTE CARLO CONSTRAINTS

We use Markov Chain Monte Carlo (MCMC) analysis to explore the joint effects of the reionization history and inflationary parameters on CMB polarization power spectra [see e.g. 42–44]. Chains of Monte Carlo samples are generated using the publicly available code CosmoMC [45] [55], which includes the code CAMB [46] for computing theoretical angular power spectra at each point in the parameter space. We have modified both codes to allow specification of an arbitrary reionization history calculated from a set of principal component amplitudes using Eq. (4), as described in [25].

For chains in which $x_e(z)$ is parametrized by its principal components, the parameters that we vary include the amplitudes of the first five components, the tensor-to-scalar ratio at $k_{\rm pivot} = 0.05$ Mpc^{-1}, and the tilt of the tensor spectrum: $\{m_1, m_2, m_3, m_4, m_5, r_{0.05}, n_t\}$. When using the simple instantaneous form of $x_e(z)$, the chain parameters are instead $\{\tau, r_{0.05}, n_t\}$ with optical depth taking the place of principal components. We compute r at $k_{\rm pivot} = 0.01$ Mpc^{-1} as a derived parameter using Eq. (2) after generating each chain.

When analyzing the parameter chains, we impose priors on the principal component amplitudes corresponding to physical values of the ionized fraction, $0 \leq x_e \leq 1$ [25]. These priors are conservative in the sense that all excluded models are unphysical, but the models we retain are not necessarily physical.

We use only polarization for parameter constraints, and assume that the values of the standard ΛCDM parameters (besides τ) are fixed by measurements of the CMB temperature anisotropies. To a good approximation the effect of $x_e(z)$ on the large-scale polarization is independent of the other parameters [25].

Specifically, we take $\Omega_b h^2 = 0.0222$, $\Omega_c h^2 = 0.106$, $100\theta = 1.04$ (corresponding to $h = 0.73$), $A_s e^{-2\tau} = 1.7 \times 10^{-9}$, and $n_s = 0.96$, consistent with the *WMAP* 3-year temperature power spectrum. When computing the optical depth to reionization we take the helium fraction to be $Y_p = 0.24$ and assume that helium is neutral. With these parameter values, the reionization optical depth out to $z_{\rm min} = 6$ is fixed at $\tau(z_{\rm min}) \approx 0.04$. The remaining contribution to the total optical depth from $z_{\rm min} < z < z_{\rm max}$ is determined by the values of $\{m_\mu\}$ for each sample in the chains. The default bin width for the fiducial models and principal components is $\Delta z = 0.25$, which is small enough that numerical effects related to binning should be negligible.

For each scenario that we study, we run four separate chains until the Gelman and Rubin convergence statistic R, corresponding to the ratio of the variance of parameters between chains to the variance within each chain, satisfies $R - 1 < 0.01$ [47, 48]. The convergence diagnostic of [49] is used to determine how much each chain must be thinned to obtain independent samples.

A. Simulated data

We use CAMB to generate model E- and B-mode polarization power spectra. We take the data to be the exact values of a given model $\hat{C}_\ell^{EE} = C_\ell^{EE}$ and $\hat{C}_\ell^{BB} = C_\ell^{BB}$, neglecting cosmic variance and noise, so we expect constraints to be centered on the fiducial parameter values rather than displaced by $\sim 1\,\sigma$. These constraints can be thought of as the average over many possible realizations of the data. (See [25] for a discussion of the effects of cosmic variance when using realizations drawn from C_ℓ instead of taking C_ℓ as the data.)

For the jth sample in a chain, the likelihood is

$$
\begin{aligned}
-\ln L_{(j)} &= \sum_{\ell=2}^{\ell_{\rm max}} \left(\ell + \frac{1}{2}\right) f_{\rm sky}^2 \\
&\times \left(\frac{\hat{\mathbf{C}}_\ell^{EE}}{\mathbf{C}_{\ell(j)}^{EE}} + \frac{\hat{\mathbf{C}}_\ell^{BB}}{\mathbf{C}_{\ell(j)}^{BB}} + \ln \frac{\mathbf{C}_{\ell(j)}^{EE}\mathbf{C}_{\ell(j)}^{BB}}{\hat{\mathbf{C}}_\ell^{EE}\hat{\mathbf{C}}_\ell^{BB}} - 2 \right),
\end{aligned}
\tag{5}
$$

where $\hat{\mathbf{C}}_\ell = \hat{C}_\ell + N_\ell$ is the sum of the simulated data and noise spectra, and $\mathbf{C}_{\ell(j)} = C_{\ell(j)} + N_\ell$ is the theoretical spectrum calculated with the parameter values at step j in the chain plus the noise spectrum. For consistency with CosmoMC, the likelihood contains an extra factor of $f_{\rm sky}$, the fraction of sky observed [56].

We set $N_\ell = 0$ to simulate measurements limited only by cosmic variance. For more realistic scenarios based on *Planck* and *CMBPol*, we model noise as

$$
N_\ell = \left(\frac{w_p^{-1/2}}{\mu\text{K-rad}} \right)^2 \exp\left[\frac{\ell(\ell+1)(\theta_{\rm FWHM}/\text{rad})^2}{8\ln 2} \right], \quad (6)
$$

where $w_p^{-1/2}$ is the polarization noise level and $\theta_{\rm FWHM}$ is the beam width.

We typically compute the likelihood up to $\ell_{\rm max} = 1000$. The E-mode spectrum and B-mode tensor spectrum are fixed at $\ell \gtrsim 100$ by setting $A_s e^{-2\tau}$ constant in the Monte Carlo chains. The impact on r and n_t constraints of the B-mode spectrum at multipoles greater than a few hundred is negligible in the presence of the lensing spectrum and experimental noise for all allowed values of r.

The fiducial reionization history is the extended, double reionization model with polarization spectra plotted in Fig. 2, for which $\tau = 0.090$. This function is chosen because it is not well described by the instantaneous reionization model, so biases due to assuming instantaneous $x_e(z)$ should be readily apparent in the parameter constraints.

We consider two fiducial values of the tensor-to-scalar ratio, $r_{0.05} = 0.3$ and $r_{0.05} = 0.03$. Using the consistency relation [Eq. (1)] to set n_t and taking the fiducial scalar tilt $n_s = 0.96$, these tensor-to-scalar ratios correspond to $r = 0.299$ and $r = 0.0283$ at $k_{\rm pivot} = 0.01$ Mpc^{-1}, respectively.

Assuming a power-law primordial spectrum, the larger fiducial tensor-to-scalar ratio, $r_{0.05} = 0.3$, is approximately the 68% upper limit on r from 3-year *WMAP*

TABLE I: Constraints on τ, r, and n_t for simulated data based on the double reionization history with optical depth $\tau^{\mathrm{fid}} = 0.09$.

$r_{0.05}^{\mathrm{fid}}$	r^{fid}	n_t^{fid}	Noise	Use PCs of $x_e(z)$?	τ	r	n_t
0.3	0.299	-0.0375	CV	Yes	0.091 ± 0.005	0.299 ± 0.004	-0.037 ± 0.018
0.3	0.299	-0.0375	CV	No	0.118 ± 0.003	0.298 ± 0.005	-0.021 ± 0.018
0.3	0.299	-0.0375	Planck	Yes	0.094 ± 0.009	0.321 ± 0.095	0.041 ± 0.196
0.3	0.299	-0.0375	Planck	No	0.113 ± 0.007	0.390 ± 0.096	0.398 ± 0.164
0.03	0.0283	-0.00375	CV	Yes	0.091 ± 0.005	0.0283 ± 0.0006	0.001 ± 0.051
0.03	0.0283	-0.00375	CV	No	0.121 ± 0.003	0.0288 ± 0.0006	0.162 ± 0.049
0.03	0.0283	-0.00375	CMBPol	Yes	0.092 ± 0.007	0.032 ± 0.009	0.069 ± 0.184
0.03	0.0283	-0.00375	CMBPol	No	0.122 ± 0.005	0.038 ± 0.010	0.491 ± 0.165

data, although when large-scale structure data are included it is ruled out at about 95% CL [9]. A tensor spectrum with this value of r should be detectable by the *Planck* satellite [12]. The smaller value of r may be out of the reach of *Planck* but accessible to a next-generation CMB satellite, such as the proposed *CMBPol* [15]. In addition to CV-limited measurements, we consider a noise spectrum based on *Planck* with sensitivity $w_p^{-1/2} = 81$ μK$'$ and beam size $\theta_{\mathrm{FWHM}} = 7.1'$ for the $r_{0.05} = 0.3$ simulated data [12, 50], and low-resolution *CMBPol*-like noise with $w_p^{-1/2} = 20$ μK$'$ and $\theta_{\mathrm{FWHM}} = 60'$ for $r_{0.05} = 0.03$ [15] (dotted curves in Fig. 2). We assume $f_{\mathrm{sky}} = 0.8$ for both *Planck* and *CMBPol* and take $f_{\mathrm{sky}} = 1$ for the more idealized, CV-limited data. In all cases we neglect foregrounds, assuming that they can be adequately subtracted using polarization data from frequency channels not used for cosmological parameter estimation.

The B-mode lensing spectrum has a significant impact on constraints on r and n_t, but including lensing significantly slows down the computation of the angular power spectra in CAMB. However, $C_\ell^{BB,\mathrm{L}}$ is nearly independent of the parameters that we vary in the Monte Carlo chains. Rather than computing the effects of lensing directly, then, we treat the lensing spectrum as a fixed contribution to the noise power spectrum. Tests comparing this approximation to an analysis including the full effects of lensing show that the constraints obtained for r and n_t are the same. Using τ-dependent lensing spectra computed for each Monte Carlo sample appears to improve the constraint on τ, but this is an artifact due to fixing $A_s e^{-2\tau}$ and other parameters that also affect $C_\ell^{BB,\mathrm{L}}$, mainly $\Omega_m h^2$ [51].

B. Results

Table I lists the 1D marginalized constraints on τ, r, and n_t from the MCMC analysis for each case study. The constraints on τ, r, and n_t are plotted in Figs. 4 and 5 as 2D contours after marginalizing over all other

parameters. The two sets of contours in each panel use the same simulated data, but different parametrizations of $x_e(z)$. For the thick contours, the five lowest-variance principal components of $x_e(z)$ are included in the Monte Carlo chains, while the thin contours come from chains that treat $x_e(z)$ as instantaneous reionization with only one parameter, τ. For the principal component chains, τ is derived from the principal component amplitudes, $\{m_\mu\}$.

Since the constraint on optical depth comes primarily from the reionization peak of the E-mode spectrum, estimates of τ in all cases in Tab. I are affected similarly by the parametrization of the reionization history. As noted in [39, 52], using the one-parameter instantaneous $x_e(z)$ when that model is not sufficient to describe the true reionization history (in this case, the double reionization history represented by the thick curves in Fig. 2) can lead to a significant bias in the constraint on τ. Using a set of principal components to parametrize $x_e(z)$ removes the bias in the optical depth [25].

The impact of the reionization history assumptions for inflationary parameters depends more strongly on the values of r and the noise. We consider first the most optimistic scenario for measurement of the B-mode tensor spectrum: a CV-limited measurement of $C_\ell^{BB,\mathrm{T}}$ with approximately the largest amplitude currently allowed, $r_{0.05} = 0.3$. With this tensor-to-scalar ratio, the tensor spectrum dominates over the B-mode lensing spectrum for $\ell \lesssim 150$ (see Fig. 2), so the recombination peak of $C_\ell^{BB,\mathrm{T}}$ is free from contamination over roughly a decade in ℓ. Moreover, the lensing spectrum may be statistically subtracted well beyond the multipole where it contributes equal power.

Since the amplitude of the tensor spectrum depends on τ, r, and n_t, we expect some degeneracy between these parameters, as described in § II. Because of this degeneracy, a bias in τ can generate biases in the inflationary parameters as well, mainly n_t (since r at $k = 0.01$ Mpc^{-1} is tightly constrained by measuring $C_\ell^{BB,\mathrm{T}}$ at $\ell \approx 100$). However, τ only affects the low-ℓ reionization peak (with our assumption that $A_s e^{-2\tau}$ is held fixed), so these biases
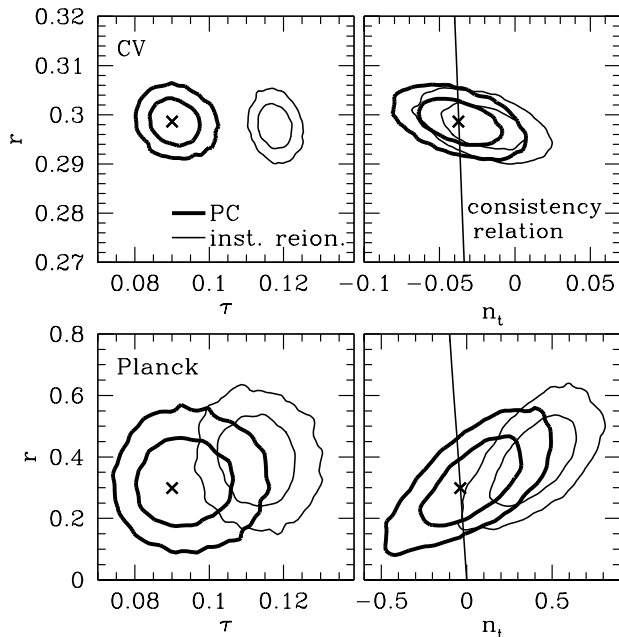
FIG. 4: 2D marginalized 68 and 95% contours for the optical depth (τ), tensor-to-scalar ratio (r), and tensor spectral index (n_t). For the simulated polarization spectra, we take $x_e(z)$ to be a double reionization history with $\tau = 0.090$ (see Fig. 2). The fiducial tensor-to-scalar ratio is set to $r_{0.05} = 0.3$ ($r = 0.299$ at $k = 0.01$ Mpc^{-1}), and the fiducial tensor tilt is assumed to obey the consistency relation, $n_t = -r/8$ (*right panels, line*). Crosses indicate these fiducial parameter values. For the thick contours, the chains include the five lowest-variance principal components of $x_e(z)$. Thin contours show the constraints when $x_e(z)$ is instead assumed to be instantaneous and parametrized only by τ. The lensing spectrum is treated as a contribution to the noise. *Top panels*: CV-limited data; *bottom*: including *Planck*-like noise.

FIG. 5: Same as Fig. 4, but with fiducial tensor-to-scalar ratio $r_{0.05} = 0.03$ ($r = 0.0283$ at $k = 0.01$ Mpc^{-1}). *Top panels*: CV-limited data; *bottom*: including *CMBPol*-like noise.

will only be significant if the reionization peak contributes significantly to constraints on the tensor spectrum. In this optimistic scenario with $r_{0.05} = 0.3$ and cosmic variance-limited measurements, enough of the tensor recombination peak is observable so that additionally measuring the reionization peak has a negligible effect on constraints on r and n_t; the values of these parameters are determined almost entirely by C_ℓ^{BB} at $20 \lesssim \ell \lesssim 500$. As a result, the bias in the inflationary parameters due to incorrectly assuming instantaneous reionization is small; as the contours in the top right panel of Fig. 4 show, the true parameter values remain within the 68% CL even with this bias.

Now consider the same tensor-to-scalar ratio but more realistic assumptions about the experimental noise. Using our assumed noise spectrum for *Planck* as described in § IV A, we find constraints on τ, r, and n_t as shown in the bottom panels of Fig. 4. The most obvious difference from the CV-limited case is that the parameter uncertainties are larger, especially for the inflationary pa-
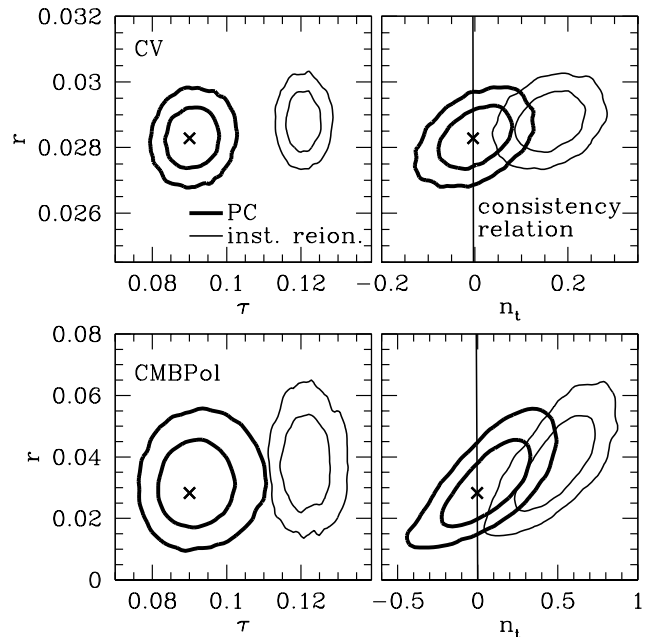
rameters. There is also a difference in the instantaneous reionization biases: while the optical depth bias is similar to the CV-limited case, n_t is biased much more with *Planck*-like noise than with a CV-limited measurement. The additional bias is due to the greater dependence on the reionization peak of $C_\ell^{BB,T}$ for n_t constraints since the noise associated with *Planck* makes measurement of the recombination peak much more difficult.

Note that while r at $k_{\rm pivot} = 0.01$ Mpc^{-1} is still determined fairly accurately in this scenario, if the tensor-to-scalar ratio were quoted elsewhere, e.g. as $r_{0.002}$ or $r_{0.05}$, a significant bias would appear in that parameter as well. For example, Fig. 6 shows that $r_{0.0007}$, normalized at the approximate scale of the reionization peak, lies significantly below the fiducial value in most of our test cases. The choice of scale also affects the uncertainty in the tensor-to-scalar ratio; while the error we quote for n_t agrees with similar studies, e.g. [31], the error on r differs in general since degeneracy with n_t due to a different choice of $k_{\rm pivot}$ can greatly increase σ_r.

With the larger bias in n_t in the presence of *Planck*-like noise, the true parameter values are excluded at the 95% CL. Moreover, the consistency relation for single-field slow-roll inflation (plotted as a line in the $r - n_t$ plots) is excluded at about the same confidence level. An incorrect assumption about the reionization history could therefore lead to wrongly rejecting the simplest class of inflationary models.

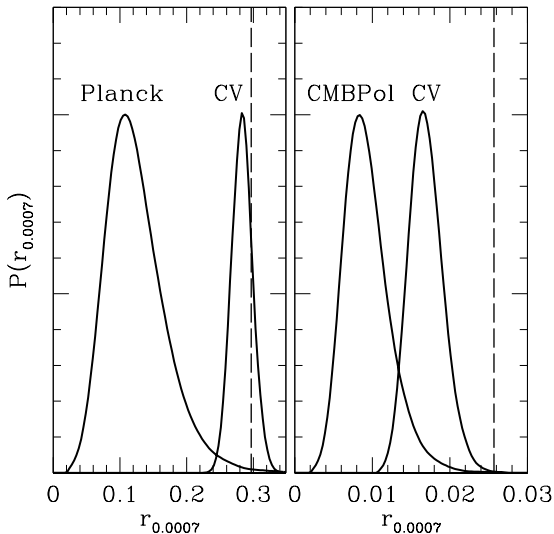As the thick contours in Fig. 4 show, when general reionization histories are considered by parametrizing

FIG. 6: 1D marginalized distributions of $r_{0.0007}$, the tensor-to-scalar ratio on scales near the reionization peak, for each of the four MCMC scenarios in Figs. 4 and 5. The fiducial values of $r_{0.0007}$ are indicated by vertical dashed lines, and the normalization is arbitrary.

$x_e(z)$ by its principal components, the biases in τ, r, and n_t are all removed. The constraints on r and n_t still may not be very strong for an experiment like *Planck*, but at least when using the principal components of $x_e(z)$ one would not be led to exclude the true underlying model of inflation. Furthermore, the precision of the constraints is not substantially degraded by the principal component parametrization.

Note that the exact magnitude and direction of the parameter biases depend on what the true reionization history actually is. The goal here is not to make specific predictions about these biases, but rather to give an idea of how large they could be and to show that they can be avoided by allowing for general models of reionization.

How does uncertainty about reionization influence constraints on inflationary parameters if the amplitude of the tensor spectrum is smaller? In general, we expect the importance of the reionization peak of $C_\ell^{BB,\mathrm{T}}$ relative to the recombination peak to increase as the tensor spectrum drops further below the dominant source of "noise" on large scales, whether that be the noise spectrum of an experiment or the B-mode lensing signal. To check this expectation, we use simulated data with a fiducial tensor-to-scalar ratio of $r_{0.05} = 0.03$. The resulting constraints on τ, r, and n_t, plotted as for the $r_{0.05} = 0.3$ results, are shown in Fig. 5 for both cosmic variance-limited measurements (top panels) and the *CMBPol*-like noise spectrum described in § IV A (bottom panels).

With a CV-limited experiment and $r_{0.05} = 0.03$, due to the greater influence of lensing relative to the tensor spectrum, the reionization peak ($\ell < 20$) and recombination peak at $\ell \lesssim 300$ contribute roughly equally to the

constraint on n_t. Because of this, assuming the wrong reionization history biases n_t more than for $r_{0.05} = 0.3$, and in this case the consistency relation would be excluded at more than the 95% CL.

If we add the *CMBPol* noise spectrum ($w_p^{-1/2} = 20\ \mu\mathrm{K}'$, $\theta_{\mathrm{FWHM}} = 60'$), both biases and errors on parameters are larger. The constraints in this case are quite similar to the constraints in the case of *Planck* with $r_{0.05} = 0.3$ (except with all r values reduced by a factor of 10), which makes sense since the low-ℓ amplitude of *CMBPol* noise relative to $C_\ell^{BB,\mathrm{T}}$ with $r_{0.05} = 0.03$ is similar to that of *Planck* noise to $C_\ell^{BB,\mathrm{T}}$ with $r_{0.05} = 0.3$ (see Fig. 2). Note that our assumptions about the *CMBPol* noise spectrum are on the conservative end of the range usually considered for such an experiment; better sensitivity ($\sim 1\ \mu\mathrm{K}'$) and/or resolution ($\sim 1 - 10$ arcmin) would enable measurement of the tensor B-modes to smaller scales so that constraints on inflationary parameters would be closer to the CV-limited scenario.

For even lower values of r than those considered here, the impact of reionization on constraints on inflationary parameters is likely to be the same or greater. Even for an idealized, cosmic variance-limited experiment, the B-mode signal due to lensing becomes a significant contaminant of $C_\ell^{BB,\mathrm{T}}$ at $r < 0.03$. Due to the shape of the spectra, if any part of $C_\ell^{BB,\mathrm{T}}$ is detectable above the lensing B-modes and noise for low tensor-to-scalar ratios it will be the reionization peak. Any bias in τ due to incorrect modeling of the reionization history will then cause the inferred value of n_t to be biased. Of course, at very low r the uncertainties are so large that the parameters are not usefully constrained at all. In this case, it may be possible to measure n_t using direct observations by future gravitational-wave experiments to better accuracy than what is possible with CMB polarization [53, 54].

Finally, note that although the choice of normalization scale $k_{\mathrm{pivot}} = 0.01\ \mathrm{Mpc}^{-1}$ is intended to decorrelate r from the other parameters, there is some remaining degeneracy with n_t. The direction of this degeneracy depends on whether or not $C_\ell^{BB,\mathrm{T}}$ can be measured on scales smaller than k_{pivot}. For CV-limited measurement of a B-mode spectrum with $r = 0.3$, these smaller scales are observable. A larger tensor tilt that increases the power at $\ell \gtrsim 100$ can be compensated for by lowering the value of r, so r and n_t are anticorrelated in this case (top right panel of Fig. 4). If the tensor spectrum on such small scales is hidden by lensing B-modes or noise, then the low-ℓ side of the recombination peak becomes more important. Increasing tensor tilt lowers the power at $20 \lesssim \ell \lesssim 100$, so r is correlated with n_t so as to match the spectrum of the data on these scales (lower right panel of Fig. 4 and right panels of Fig. 5).

V. DISCUSSION

The value of the optical depth to reionization estimated from the CMB E-mode polarization spectrum on large scales can be biased by adopting a model that has insufficient freedom to describe the true reionization history. Likewise, the use of simple reionization models can bias inflationary parameters such as the tensor-to-scalar ratio and tensor tilt that depend on the large-scale amplitude of the B-mode spectrum of primordial gravitational waves. In each case, the problem can be solved by using a more general parametrization of the reionization history. We have shown that using a small but complete set of the principal components of the reionization history effectively yields unbiased constraints on both reionization and inflationary parameters.

Measurements of r and n_t are only affected by the assumed form of the reionization history if the reionization peak of the tensor B-mode spectrum at the very largest scales is needed to precisely constrain the parameters. If, instead, good constraints can be obtained using only the B-mode recombination peak at intermediate scales, then assumptions about reionization do not affect tests of the consistency relation between r and n_t. They would instead appear as false evidence for running of the tensor tilt in violation of slow-roll expectations. Measurement of the recombination peak however is inhibited by experimental noise and contamination from E-mode power converted to B-mode power by gravitational lensing, both of which become more important at smaller scales.

To study the potential impact of reionization on parameter constraints from B-mode polarization, we have employed a Markov Chain Monte Carlo analysis of simulated CMB polarization power spectra and compared results for two descriptions of reionization: a simple, one-parameter, instantaneous reionization model, and a parametrization using principal components of the reionization history with respect to the E-mode polarization power spectrum.

By varying the properties of the simulated polariza-tion power spectra, including the fiducial tensor-to-scalar ratio and the noise spectrum, we have determined over what range of scales CMB polarization data is most important for constraining inflationary parameters in various scenarios. In particular, the question of whether the large-scale reionization peak of $C_\ell^{BB,T}$ or the smaller-scale recombination peak is more important determines the severity of bias in inflationary parameters when reionization is modeled incorrectly.

If the tensor-to-scalar ratio is near the current upper limit of $r \sim 0.3$ and measurements of B-mode polarization are limited only by cosmic variance, then the spectrum on scales $20 \lesssim \ell \lesssim 500$ dominates constraints on r and n_t and incorrect assumptions about reionization do not strongly bias the results. If the true tensor-to-scalar ratio is more than a factor of a few smaller than this upper bound, however, then lensing B-modes limit the information that can be extracted from the recombination peak of the tensor spectrum alone. Furthermore, all-sky experiments in the foreseeable future are likely to have noise that exceeds the lensing signal, making tests of inflation even more reliant on the reionization peak of the tensor B-modes on large scales. In all of these cases, a general parametrization of reionization such as that provided by principal components allows the use of the B-mode reionization peak for inflationary parameter constraints without significantly worsening the errors on those parameters.

[1] A. H. Guth, Phys. Rev. D **23**, 347 (1981).
[2] A. Albrecht and P. J. Steinhardt, Physical Review Letters **48**, 1220 (1982).
[3] A. D. Linde, Physics Letters B **108**, 389 (1982).
[4] K. Sato, Mon. Not. R. Astron. Soc. **195**, 467 (1981).
[5] W. Hu and M. White, Phys. Rev. Lett. **77**, 1687 (1996), `arXiv:astro-ph/9602020`.
[6] D. N. Spergel and M. Zaldarriaga, Physical Review Letters **79**, 2180 (1997), `arXiv:astro-ph/9705182`.
[7] W. Hu, D. N. Spergel, and M. White, Phys. Rev. D **51**, 3288 (1997), `arXiv:astro-ph/9605193`.
[8] H. V. Peiris, E. Komatsu, L. Verde, D. N. Spergel, C. L. Bennett, M. Halpern, G. Hinshaw, N. Jarosik, A. Kogut, M. Limon, et al., Astrophys. J. Suppl. Ser. **148**, 213 (2003), `arXiv:astro-ph/0302225`.

[9] D. N. Spergel, R. Bean, O. Doré, M. R. Nolta, C. L. Bennett, J. Dunkley, G. Hinshaw, N. Jarosik, E. Komatsu, L. Page, et al., Astrophys. J. Suppl. Ser. **170**, 377 (2007), `arXiv:astro-ph/0603449`.
[10] M. Kamionkowski, A. Kosowsky, and A. Stebbins, Physical Review Letters **78**, 2058 (1997), `arXiv:astro-ph/9609132`.
[11] U. Seljak and M. Zaldarriaga, Physical Review Letters **78**, 2054 (1997), `arXiv:astro-ph/9609169`.
[12] The Planck Collaboration (2006), `arXiv:astro-ph/0604069`.
[13] P. Oxley, P. A. Ade, C. Baccigalupi, P. deBernardis, H.-M. Cho, M. J. Devlin, S. Hanany, B. R. Johnson, T. Jones, A. T. Lee, et al., in *Infrared Spaceborne Remote Sensing XII, Proceedings of the SPIE*, edited by M. Stro-

jnik (2004), vol. 5543, pp. 320–331, `arXiv:astro-ph/0501111`.

[14] K. W. Yoon, P. A. R. Ade, D. Barkats, J. O. Battle, E. M. Bierman, J. J. Bock, J. A. Brevik, H. C. Chiang, A. Crites, C. D. Dowell, et al., in *Millimeter and Submillimeter Detectors and Instrumentation for Astronomy III, Proceedings of the SPIE*, edited by J. Zmuidzinas, W. S. Holland, S. Withington, and W. D. Duncan (2006), vol. 6275, `arXiv:astro-ph/0606278`.

[15] J. Bock et al. (2006), `arXiv:astro-ph/0604101`.

[16] B. Maffei, P. A. R. Ade, C. Calderon, A. D. Challinor, P. de Bernardis, L. Dunlop, W. K. Gear, Y. Giraud-Héraud, D. J. Goldie, K. J. B. Grainge, et al., in *EAS Publications Series* (2005), pp. 251–256.

[17] C. R. Lawrence, T. C. Gaier, and M. Seiffert, in *Millimeter and Submillimeter Detectors for Astronomy II, Proceedings of the SPIE*, edited by C. M. Bradford, P. A. R. Ade, J. E. Aguirre, J. J. Bock, M. Dragovan, L. Duband, L. Earle, J. Glenn, H. Matsuhara, B. J. Naylor, et al. (2004), vol. 5498, pp. 220–231.

[18] C. J. MacTavish, P. A. R. Ade, E. S. Battistelli, S. Benton, R. Bihary, J. J. Bock, J. R. Bond, J. Brevik, S. Bryan, C. R. Contaldi, et al. (2007), `arXiv:0710.0375`.

[19] J. Ruhl, P. A. R. Ade, J. E. Carlstrom, H.-M. Cho, T. Crawford, M. Dobbs, C. H. Greer, N. w. Halverson, W. L. Holzapfel, T. M. Lanting, et al., in *Millimeter and Submillimeter Detectors for Astronomy II, Proceedings of the SPIE*, edited by C. M. Bradford, P. A. R. Ade, J. E. Aguirre, J. J. Bock, M. Dragovan, L. Duband, L. Earle, J. Glenn, H. Matsuhara, B. J. Naylor, et al. (2004), vol. 5498, pp. 11–29, `arXiv:astro-ph/0411122`.

[20] A. Kogut et al., New Astron. Rev. **50**, 1009 (2006), `arXiv:astro-ph/0609546`.

[21] G. Polenta, P. A. R. Ade, J. Bartlett, E. Bréelle, L. Conversi, P. de Bernardis, C. Dufour, M. Gervasi, M. Giard, C. Giordano, et al., New Astronomy Review **51**, 256 (2007).

[22] M. Zaldarriaga, Phys. Rev. D **55**, 1822 (1997), `arXiv:astro-ph/9608050`.

[23] L. Page, G. Hinshaw, E. Komatsu, M. R. Nolta, D. N. Spergel, C. L. Bennett, C. Barnes, R. Bean, O. Doré, J. Dunkley, et al., Astrophys. J. Suppl. Ser. **170**, 335 (2007), `arXiv:astro-ph/0603450`.

[24] G. P. Holder, Z. Haiman, M. Kaplinghat, and L. Knox, Astrophys. J. **595**, 13 (2003), `arXiv:astro-ph/0302404`.

[25] M. J. Mortonson and W. Hu, Astrophys. J. (in press) (2007), `arXiv:0705.1132`.

[26] B. Keating and N. Miller, New Astronomy Review **50**, 184 (2006), `arXiv:astro-ph/0508269`.

[27] W. Hu and G. P. Holder, Phys. Rev. D **68**, 023001 (2003), `arXiv:astro-ph/0303400`.

[28] J. E. Lidsey, A. R. Liddle, E. W. Kolb, E. J. Copeland, T. Barreiro, and M. Abney, Reviews of Modern Physics **69**, 373 (1997), `arXiv:astro-ph/9508078`.

[29] M. Zaldarriaga and U. Seljak, Phys. Rev. D **58**, 023003 (1998), `arXiv:astro-ph/9803150`.

[30] M. Bowden, A. N. Taylor, K. M. Ganga, P. A. R. Ade, J. J. Bock, G. Cahill, J. E. Carlstrom, S. E. Church, W. K. Gear, J. R. Hinderks, et al., Mon. Not. R. Astron. Soc. **349**, 321 (2004), `arXiv:astro-ph/0309610`.

[31] L. Verde, H. V. Peiris, and R. Jimenez, Journal of Cosmology and Astro-Particle Physics **1**, 19 (2006), `arXiv:astro-ph/0506036`.

[32] M. Tucci, E. Martínez-González, P. Vielva, and J. Delabrouille, Mon. Not. R. Astron. Soc. **360**, 935 (2005), `arXiv:astro-ph/0411567`.

[33] A. Amblard, A. Cooray, and M. Kaplinghat, Phys. Rev. D **75**, 083508 (2007), `arXiv:astro-ph/0610829`.

[34] W. Hu and T. Okamoto, Astrophys. J. **574**, 566 (2002), `arXiv:astro-ph/0111606`.

[35] L. Knox and Y.-S. Song, Phys. Rev. Lett. **89**, 011303 (2002), `arXiv:astro-ph/0202286`.

[36] M. Kesden, A. Cooray, and M. Kamionkowski, Phys. Rev. Lett. **89**, 1304 (2002).

[37] U. Seljak and C. M. Hirata, Phys. Rev. **D69**, 043005 (2004), `arXiv:astro-ph/0310163`.

[38] L. Marian and G. M. Bernstein (2007), `arXiv:0710.2538`.

[39] M. Kaplinghat, M. Chu, Z. Haiman, G. P. Holder, L. Knox, and C. Skordis, Astrophys. J. **583**, 24 (2003), `arXiv:astro-ph/0207591`.

[40] L. P. L. Colombo, G. Bernardi, L. Casarini, R. Mainini, S. A. Bonometto, E. Carretti, and R. Fabbri, Astron. Astrophys. **435**, 413 (2005), `arXiv:astro-ph/0408022`.

[41] W. Hu and M. White, Phys. Rev. D **56**, 596 (1997), `arXiv:astro-ph/9702170`.

[42] N. Christensen, R. Meyer, L. Knox, and B. Luey, Class. Quant. Grav. **18**, 2677 (2001), `arXiv:astro-ph/0103134`.

[43] A. Kosowsky, M. Milosavljevic, and R. Jimenez, Phys. Rev. **D66**, 063007 (2002), `arXiv:astro-ph/0206014`.

[44] J. Dunkley, M. Bucher, P. G. Ferreira, K. Moodley, and C. Skordis, Mon. Not. Roy. Astron. Soc. **356**, 925 (2005), `arXiv:astro-ph/0405462`.

[45] A. Lewis and S. Bridle, Phys. Rev. D **66**, 103511 (2002), `arXiv:astro-ph/0205436`.

[46] A. Lewis, A. Challinor, and A. Lasenby, Astrophys. J. **538**, 473 (2000), `arXiv:astro-ph/9911177`.

[47] A. Gelman and D. B. Rubin, Statistical Science **7**, 457 (1992), ISSN 0883-4237.

[48] S. P. Brooks and A. Gelman, Journal of Computational and Graphical Statistics **7**, 434 (1998), ISSN 1061-8600.

[49] A. E. Raftery and S. M. Lewis, in *Bayesian Statistics*, edited by J. M. Bernado (OUP, 1992), p. 765.

[50] A. Albrecht, G. Bernstein, R. Cahn, W. L. Freedman, J. Hewitt, W. Hu, J. Huth, M. Kamionkowski, E. W. Kolb, L. Knox, et al. (2006), `arXiv:astro-ph/0609591`.

[51] K. M. Smith, W. Hu, and M. Kaplinghat, Phys. Rev. D **74**, 123002 (2006), `arXiv:astro-ph/0607315`.

[52] A. Lewis, J. Weller, and R. Battye, Mon. Not. R. Astron. Soc. **373**, 561 (2006), `arXiv:astro-ph/0606552`.

[53] S. Chongchitnan and G. Efstathiou, Phys. Rev. D **73**, 083511 (2006), `arXiv:astro-ph/0602594`.

[54] T. L. Smith, H. V. Peiris, and A. Cooray, Phys. Rev. D **73**, 123503 (2006), `arXiv:astro-ph/0602137`.

[55] `http://cosmologist.info/cosmomc/`

[56] The extra factor of f_{sky} is meant to approximately model the loss of information due to mode coupling with incomplete sky coverage, but the correct approach depends on the nature of the information extracted.